Spectrochimica Acta Part B 64 (2009) 147–154

Contents lists available at ScienceDirect

Spectrochimica Acta Part B

journal homepage: www.elsevier.com/locate/sab

Double pulse laser induced breakdown spectroscopy: Experimental study of lead emission intensity dependence on the wavelengths and sample matrix

V. Piscitelli S [a], M.A. Martínez L. [a], A.J. Fernández C. [a], J.J. González [b], X.L. Mao [b], R.E. Russo [b,*]

[a] Laboratorio de Espectroscopia Láser, Escuela de Química, Facultad de Ciencias, Universidad Central de Venezuela, Caracas, DC 1020, Venezuela
[b] Lawrence Berkeley National Laboratory, Berkeley, CA 94720, USA

ARTICLE INFO

Article history:
Received 9 May 2008
Accepted 23 November 2008
Available online 3 December 2008

Keywords:
Double pulse LIBS
Lead
Laser induced breakdown spectroscopy

ABSTRACT

Lead (Pb) emission intensity (atomic line 405.78 nm) dependence on the sample matrix (metal alloy) was studied by means of collinear double pulse (DP)-laser induced breakdown spectroscopy (LIBS). The measurement of the emission intensity produced by three different wavelength combinations (i.e. I:532 nm–II:1064 nm, I:532 nm–II:532 nm, and I:532 nm–II:355 nm) from three series of standard reference materials showed that the lead atomic line 405.78 nm emission intensity was dependent on the sample matrix for all the combination of wavelengths, however reduced dependency was found for the wavelength combination I:532 nm–II:355 nm.

Two series of standard reference materials from the National Institute of Standards and Technology (NIST) and one series from the British Chemical Standards (BCS) were used for these experiments. Calibration curves for lead ablated from NIST 626–630 ("$Zn_{95}Al_4Cu_1$") provided higher sensitivity (slope) than those calibration curves produced from NIST 1737–1741 ("$Zn_{99.5}Al_{0.5}$") and with the series BCS 551–556 ("$Cu_{87}Sn_{11}$"). Similar trends between lead emission intensity (calibration curve sensitivities) and reported variations in plasma temperatures caused by the differing ionization potentials of the major and minor elements in these samples were established.

1. Introduction

Laser-induced breakdown spectroscopy has become a viable technology for elemental analysis of solid samples. This technology is based on the spectral emission from an induced plasma created when an intense laser pulse is focused onto a sample. LIBS advantages are that it allows direct, *in situ*, and rapid chemical analysis with little or no sample preparation [1–5]. Moreover, LIBS has been shown to provide suitability for remote chemical analysis of hazardous or difficult-to-reach samples [6–9]. Nevertheless, there are several areas to address for LIBS to become a more dominant technology for spectroscopic analysis. Among these areas are quantification (matrix-matched requirements, etc), and performance metrics (accuracy, precision, limit of detection, etc.) as compared to other analytical techniques such as Inductively Coupled Plasma–Mass Spectrometry (ICP–MS), and Atomic Emission Spectroscopy (AES). Research efforts have been directed to reduce or eliminate matrix dependence and improve the analytical figures of merit. One of the approaches to achieve these goals has been the use of multiple laser pulses. In particular, the use of two laser pulses has received a great deal of attention in recent years. Improvements in analytical figures of merit by double pulse-LIBS compared to single pulse-LIBS, have been described by several authors [10–22]. The term double pulse-LIBS is defined as two laser pulses, from two different sources (commonly) that are separated in time by nanosecond or microsecond time delay.

Several DP-LIBS configurations have been studied using both orthogonal and collinear configurations. In the orthogonal configuration, the two laser pulses are 90° with respect to each other. Depending on which of the laser pulses first reaches the surface (as selected by the user), two situations have been explored. In one, the first laser pulse is used to ablate the sample and create a rarefied ambient for the second laser pulse. Alternatively, the first laser pulse is used to create a spark above the sample surface to also generate a rarified ambient in which the plasma generated by the second laser pulse can expand to a larger size [17,21,23,24]. In the collinear configuration as used in this study, both laser pulses travel the same path.

These two configuration have been successfully used to increase sensitivity for the analysis of liquids [25], solids immersed in liquids [26], and a variety of solid samples [27]. The enhancement in spectral line emission intensity using DP excitation depends on several parameters. Among these parameters are: plasma density, laser wavelength, inter-pulse delay time, line excitation energy, etc. The enhancement is proposed to be due to higher plasma temperature and/or larger and longer plasma duration, as well as in some cases, to increased ablated mass [17,19,20,24,27,28].

* Corresponding author.
E-mail address: RERusso@lbl.gov (R.E. Russo).

0584-8547/$ – see front matter © 2008 Elsevier B.V. All rights reserved.
doi:10.1016/j.sab.2008.11.008

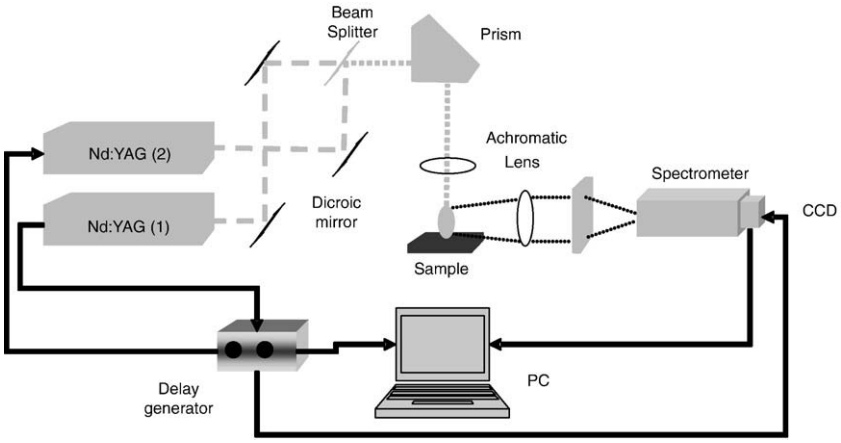

Fig. 1. Experimental setup.

Lead is recognized worldwide as a hazardous metal. Increased awareness and public interest in the health risks associated with this toxic metal often necessitates the determination of this element in environmental, biological, food, manufacturing materials (for example plastic materials used in the fabrication of toys), and geological samples. Some of these samples represent an immense challenge for traditional wet analytical techniques due to the difficulty of sample preparation. Studies addressing the ability to determine metals concentration directly from any sample, with no or little sample preparation will contribute to the improved monitoring of toxic metals such as lead.

Several quantification methods have been proposed for chemical analysis using LIBS to replace the use of calibration curves as the primary method of quantification [8,29–35]. For the most part, the reason is due to the lack of standard reference materials for most samples, and in some cases, due to limited knowledge of the sample of interest. However, calibration curves are the best method for quantitative chemical analysis; they provide an empirical relationship that encloses a large number of variables and are the simplest way to account for all factors that influence an analytical measurement. In this paper the study of LIBS performance metrics is provided based on calibration curves produced by the lead emission intensity (atomic line 405.78 nm) from metal alloy samples. Precision, sensitivity and limit of detection (defined as the concentration calculated using calibration curve intercept+3*standard deviation of the intercept) by DP-LIBS (using different wavelength combinations) in a collinear arrangement compared to SP-LIBS is presented.

2. Experimental

An experimental diagram for the double pulse LIBS system is shown in Fig. 1. Two Nd:YAG lasers system (10 Hz, 8 ns, Surelite I and II, from Continuum) were arranged in a collinear configuration, directed by a dichroic mirror to a sample at ambient pressure. The wavelength of the first laser was fixed at 532 nm and the second laser pulse wavelength was switched between 1064, 532 and 355 nm (fundamental, second and third harmonics). Both laser beams were focused onto the sample with an achromatic quartz lens (200 mm focal length) to a 500 μm spot size. The focal point was located 1 mm below the sample surface in order to avoid air breakdown above the sample surface.

A cylindrical quartz lens was used to image the laser-induced plasma onto the entrance slit of a Czerny-Turner spectrometer (Spex 500 M) equipped with a 3600 groove/mm grating. Spectral emission was detected by a Charge Coupled Device system (CCD) 512×122 pixels (Hamamatsu, C7041) using 20 ms integration starting from the last laser pulse (second pulse in the double pulse mode). Independent firing of the two laser pulses was achieved by an external delay generator providing time between laser pulses from 0 to 200 μs.

Three sets of standard reference materials from the National Institute of Standards and Technology (NIST) and British Chemical Standards (BCS) were used for these experiments. These standards series were: Zinc-Based Die-Casting Alloy NIST 626–630 ("$Zn_{95}Al_4Cu_1$"), Zinc–Aluminum Alloy NIST ("$Zn_{99.5}Al_{0.5}$"), and Bronzes ("$Cu_{87}Sn_{11}$"). The certified compositions for these series are listed in Tables 1 and 2. Lead has a certified composition over a wide concentration range in the standard reference materials chosen for this study. The lead atomic line at 405.78 nm was selected since it is one of the most intense emission lines and spectral interference was not observed.

3. Results and discussions

3.1. Single pulse mode (SP-LIBS)

Single pulse LIBS experiments were carried out by collecting the spectral emission generated by 100 laser pulses using a 20 ms integration time. Each measurement was made on a fresh surface, and the

Table 1
Certificated composition of the standards series NIST 626–630 and NIST 1737–1741

SRM	Cu	Al	Mg	Fe	Pb	Cd	Sn	Cr	Mn	Ni	Si	Zn
NIST 626	0.056	3.56	0.02	0.103	0.0022	0.0016	0.0012	0.0395	0.048	0.047	0.042	96.1355
NIST 627	0.132	3.88	0.03	0.023	0.0082	0.0051	0.0042	0.0038	0.014	0.0029	0.021	96.0078
NIST 628	0.611	4.59	0.0094	0.066	0.0045	0.004	0.0017	0.0087	0.0091	0.03	0.008	95.2686
NIST 629	1.5	5.15	0.094	0.017	0.0135	0.0155	0.012	0.0008	0.0017	0.0075	0.078	93.1100
NIST 630	0.976	4.3	0.03	0.023	0.0083	0.0048	0.004	0.0031	0.0106	0.0027	0.022	95.5915
NIST 1737		0.6302			0.0029							99.3669
NIST 1738		0.1014			0.0101							99.8885
NIST 1739		0.2049			0.0302							99.7649
NIST 1740		0.4177			0.0691							99.5132
NIST 1741		0.5242			0.1571							99.3187

Elemental composition (mass fraction, in %).

Table 2
Calibration curve parameters and limit of detection (L.O.D.) for the single pulse (SP-) and double pulse (DP-) LIBS approaches of the series NIST1737–1741

SRM	Cu	Al	P	Fe	Pb	Sn	Ni	Si	Zn
BCS551	87.4	0.052	1.01	0.2	0.8	8.92	0.76	0.018	0.74
BCS552	87.7	0.023	0.77	0.1	0.63	9.78	0.56	0.019	0.35
BCS553	87	0.017	0.68	0.056	0.47	10.8	0.44	0.022	0.49
BCS554	87.4	0.005	0.41	0.022	0.34	11.3	0.22	0.038	0.22
BCS555	87.1	<0.005	0.18	0.01	0.24	12.1	0.11	0.036	0.16
BCS556	86.4	<0.005	0.1	0.004	0.16	13.2	0.0014	<0.005	0.09

Table 3
Calibration curve parameters and limit of detection (L.O.D.) for the DP-LIBS approach of the series NIST1737–1741 and NIST 626–630

Wavelength	slope±sd	*r*	L.O.D (%)	Mode	RM's
1064	2047±736	0.9620	0.0912	SP	1737–1741
532	7654±566	0.9981	0.0135	SP	1737–1741
355	14193±734	0.9987	0.0110	SP	1737–1741
532-532	34154±1306	0.9924	0.0027	DP	1737–1741

average of the measurements was calculated. Due to the limited bandwidth of the spectrometer, no other spectral lines were acquired and therefore no internal standard was used.

Calibration curves for lead in the SP-LIBS configuration using laser energy of 80 mJ and wavelengths 1064, 532 and 355 nm for the standard series NIST 1737–1742 are shown in Fig. 2. The inset figure shows the same data points plotted on a log–log scale. Significant differences in the sensitivity and detection limits of the standard series NIST 1737–1742 were obtained for the three laser wavelengths investigated. The sensitivity obtained when using 355 nm was 2 and 7 times better than the sensitivity obtained for 532 and 1064 nm, respectively. The same trend was obtained for the limit of detection, Table 3. The amount of ablated mass and plasma properties is influenced by the laser-beam parameters, and the sample properties. Studies have shown that wavelength is one of the most critical parameters affecting the nanosecond laser ablation behavior and plasma formation. It was reported that mass ablation rate at UV wavelength 266 nm is more than one order of magnitude higher compared to the infrared wavelength 1064 nm [36,37]. Among the reasons for this behavior is the fact that UV wavelengths offer higher photon energies for bond breaking and ionization that infrared wavelengths (i.e. 355 nm (3.49 eV), 532 nm (2.32 eV), and 1064 nm (1.16 eV)), another suggested reason is that there is a stronger plasma shielding at infrared wavelength, leaving less total laser energy available to interact with the target [38].

Plasma shielding refers to the process in which part of the laser beam is partially absorbed before it reaches the sample, the absorption process could involve three mechanisms; electro-neutral and electro-ion inverse Bremsstrahlung, and photo-ionization of excited atoms. A description of these mechanisms and their influence in laser ablation can be found in Bogaerts et al. [38]. Bogaerts et al.[38]

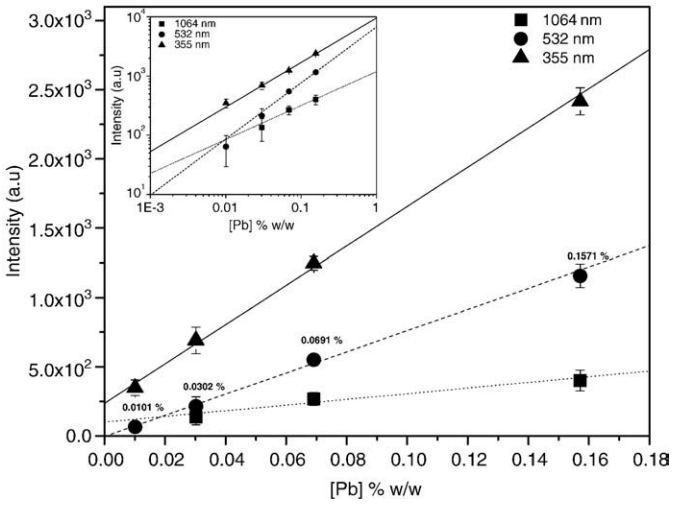

Fig. 2. Calibration curves in single pulse mode (SP) for standard reference series NIST 1737–1741.

predicted higher percentage of absorption by the induced plasma for 266 nm compared to 1064 nm in contradiction with other reports [37,39]. They reported e-n IB to be the dominant absorption mechanism for 266 nm, while the dominant absorption mechanism for 1064 nm was found to be e-i IB. They concluded that at 1064 nm the plasma absorption is much lower than a 266 nm and 532 nm at the same irradiance, despite the fact the e-i IB absorption coefficient is significantly higher. However, at 1064 nm there is much lower density of electrons, ions and neutrals in the plasma because of the much lower amount of evaporation. If Bogaerts et al.'s [38] prediction is correct 355 nm should generate a plasma with higher temperature compared to 532 nm and 1064 nm which will have an effect on analytical sensitivity, since an increase in the plasma temperature is accompanied by an increase in the number of excited species emitting from the plasma. Therefore 355 nm should provide the highest sensitivity, whereas 1064 nm should provide the lowest sensitivity for single pulse LIBS.

From Table 3, sensitivity (calibration curve slope) for 1064 nm was the lowest and that for 355 nm was the highest confirming the prediction by Bogaerts et al [38]. Also as expected under these assumptions the data obtained by using the wavelength 532 nm provided sensitivity in between the values for 1064 and 355 nm, 3.5 times higher that 1064 nm and 2 times lower that 355 nm, which seems to be due to a combination of absorption mechanisms also predicted in Bogaerts et al.'s [38] study. This wavelength was selected as the first pulse in the double pulse mode studies reported in the next section.

3.2. Double pulse mode

3.2.1. Optimization of inter-pulse separation time and energies

The optimal separation time between the two laser pulses was found by plotting LIBS emission intensity enhancement versus the delay time for the lead (Pb I) atomic line at 405.78 nm. Similar data were measured for all wavelength combinations used in this study. The lasers energies were fixed at 40 mJ (total laser energy: laser I+ Laser II=80 mJ). The sample was NIST 1741. At $\Delta t = 0$, both lasers were fired at the same time; the delay time then was varied from 0 to 10 μs. The maximum enhancement of the atomic emission intensity was measured between 5 to 10 μs with a maximum in 7.4 μs. These data support previous studies on DP-LIBS using collinear configurations [20,27].

3.2.2. Calibration curves

Calibration curves were produced for lead (405.78 nm) using the two series of NIST standard reference materials. For these experiments, different wavelengths were used for laser II (second pulse) while laser I was kept at 532 nm. The combinations of wavelengths used were: I:532 nm–II:1064 nm; I:532 nm–II:532 nm, and I:532 nm–II:355 nm. Laser energy combinations of $E_1 = 40$ mJ and $E_2 = 40$ mJ, with delay time between pulses of 7.4 μs. Similar to the SP-mode presented above, the DP-mode emission intensity was obtained from a collection of 100 spectra, each one from a fresh surface to avoid effects of fractionation due crater formation.

Fig. 3 shows two spectra which demonstrate the emission enhancement when comparing SP-LIBS (532 nm, 80 mJ) to DP-LIBS (532 nm–532 nm, 40 mJ–40 mJ), using sample NIST 1741. Fig. 4 shows

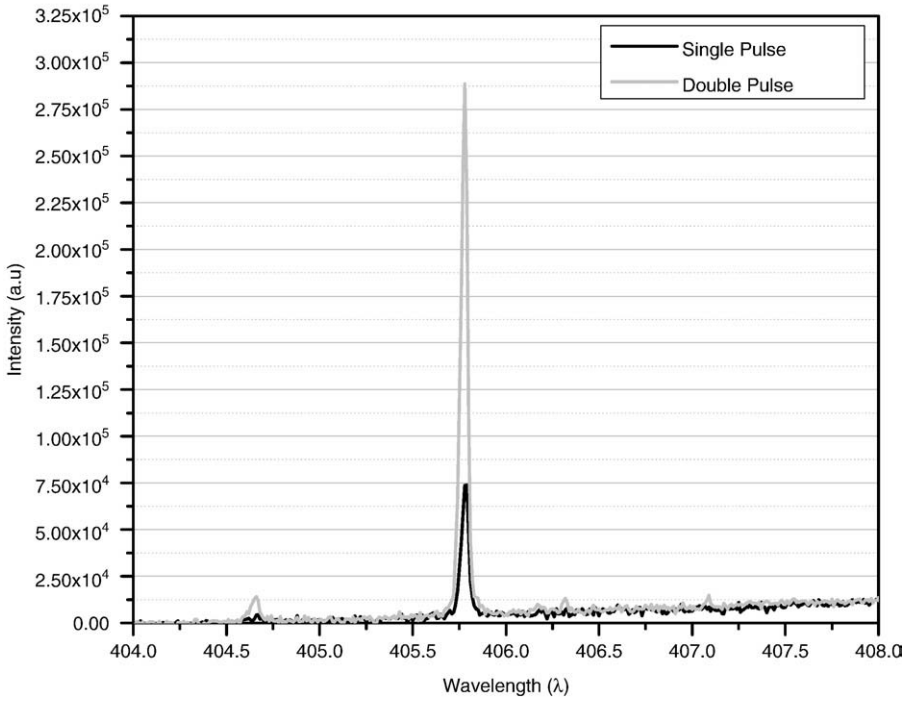

Fig. 3. Sample NIST1741-single pulse 532 nm (80 mJ)-double pulse 532–532 nm (40 mJ each).

that by using the double pulse (DP) mode, an increase in sensitivity, and enhancement of the integrated emission intensity (~4 times) were obtained compared to the SP configuration. The limit of detection showed an improvement of about five times compared to SP-mode, Table 3.

Fig. 5 shows calibration curves produced by the double pulse mode using the three combinations of laser wavelengths on the two series of standard reference materials [*a)* NIST 626–630 and *b)* NIST 1737–1741]. Higher sensitivity is evident, for the two series of NIST standard reference materials, when using the wavelength combination I:532 nm–II:1064 nm. In this case, and due to inter pulse delay time used (7.4 μs) the sample surface after the first pulse has enough time to reach the equilibrium with the environment. However, that environment temperature is that of the SP-LIBS after the considered inter pulse delay close to the target and in this case still high enough to considerably change the sample optical properties. And as was discussed above in the SP-LIBS case [40] since the plasma absorption is more efficient for shorter wavelength, the 1064 nm laser radiation, as second pulse, has a higher effective fluence on the sample surface with respect of 532 and 355 nm, leading to a higher number of ejected emitters. However, larger errors (poor reproducibility, measured as %RSD) are associated with the values measured from this combination. The combination of wavelengths I:532 nm–II:355 nm provides the lowest errors (%RSD) among the three wavelengths combinations, possibly due to more reproducible and controlled ablation event by the second pulse. In Table 4, sensitivity and limit of detection are presented for each combination of wavelengths and for each series of NIST standard reference materials. In general, the limit of detection improved one order of magnitude and sensitivity doubled compared to the single pulse approach.

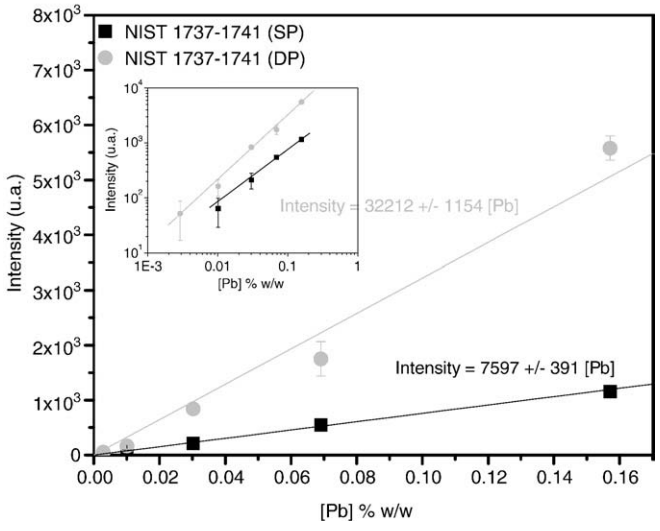

Fig. 4. Lead (Pb) calibration curves series 1737–1741. (Inset shows a log–log plot of the same data).

To evaluate the effect of the double pulse on matrix-match dependency, both NIST standard reference materials were plotted together to establish extended calibration curves. Fig. 6a, b and c show the calibration curves for each combination of wavelengths, and the highlighted region (zoom in) shows the differences between the slopes of the calibration curves obtained for each NIST standard series individually. It is evident from these plots that even samples that possess similar matrices i.e. NIST 625–630 ("$Zn_{95}Al_4Cu_1$") and 1737–1741 ("$Zn_{99.5}Al_{0.5}$") cannot be combined in order to establish extended calibration curves under these experimental conditions. However, a reduction of the matrix dependence (based on the higher correlation coefficient of the calibration curve using both series) was obtained by using the combination of wavelengths: I:532 nm–II:355 nm (r=0.9904), Fig. 7. The correlation coefficient decreased with the increase of the second pulse wavelength: I:532 nm–II532 nm (r=0.9829), and I:532 nm–II1064 nm (r=0.9716).

The matrix effect is referred as changes in analyte emission intensity, both from changes in induced plasma parameters, and/or due to changes in the laser-material interaction due to physical and chemical properties of the sample. In this case, even though the standard reference materials used in this study posses similar matrices (the major

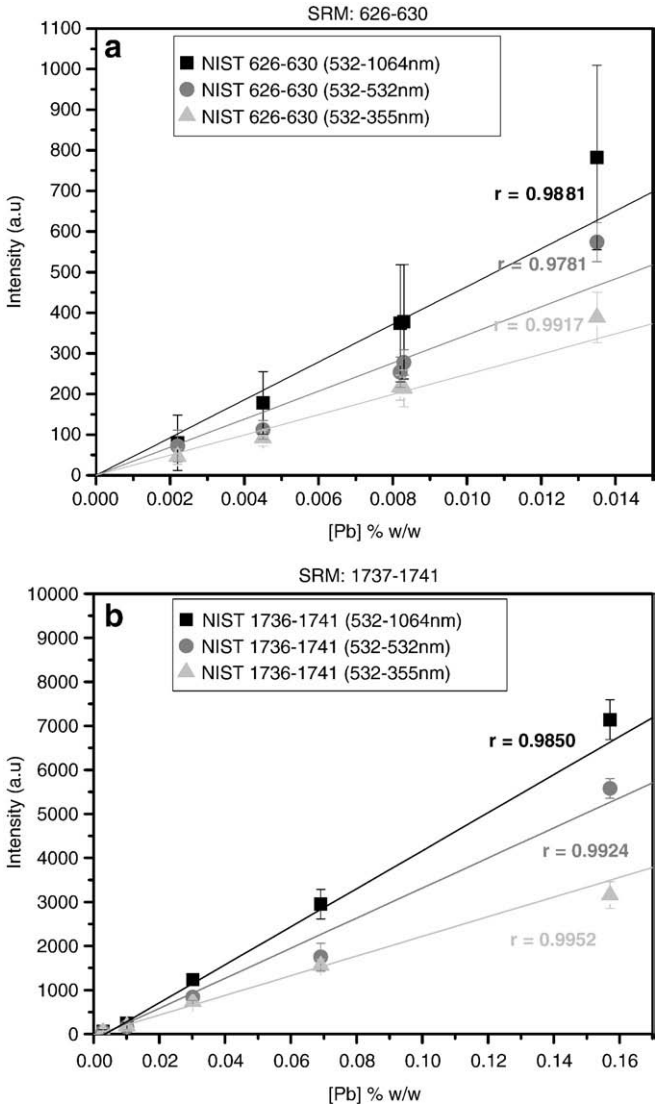

Fig. 5. Lead (Pb) calibration curves from each of the alloy standard series using double pulse mode (signals are the average of 100 measurements).

element in both series is zinc, NIST 625–630 ("$Zn_{95}Al_4Cu_1$") and 1737–1741 ("$Zn_{99.5}Al_{0.5}$")), these data demonstrate that small amounts of other constituents, in particular minor elements such as aluminum and copper, could affect plasma properties. These changes in plasma properties could be beneficial or detrimental to the emission of a particular element, as shown by Ismail et al [41], where different detection limits and precision were reported for the same element in different matrices.

Table 4
Certificated composition of the standards series BCS 551–556

Wavelength	slope±sd	r	L.O.D (%)	Mode	RM's
532-1064	43191±2245	0.9850	0.0019	DP	1737–1741
532-1064	55270±15621	0.9881	0.0046	DP	626–630
532-532	34154±1306	0.9924	0.0027	DP	1737–1741
532-532	44096±4641	0.9781	0.0023	DP	626–630
532-355	22335±1315	0.9952	0.0037	DP	1737–1741
532-355	29372±4199	0.9917	0.0024	DP	626–630
532-1064	42043±2177	0.9716	0.0018	DP	17xx–6xx
532-532	34217±1235	0.9829	0.0014	DP	17xx–6xx
532-355	22692±129	0.9904	0.0017	DP	17xx–6xx

Elemental composition (mass fraction, in %).

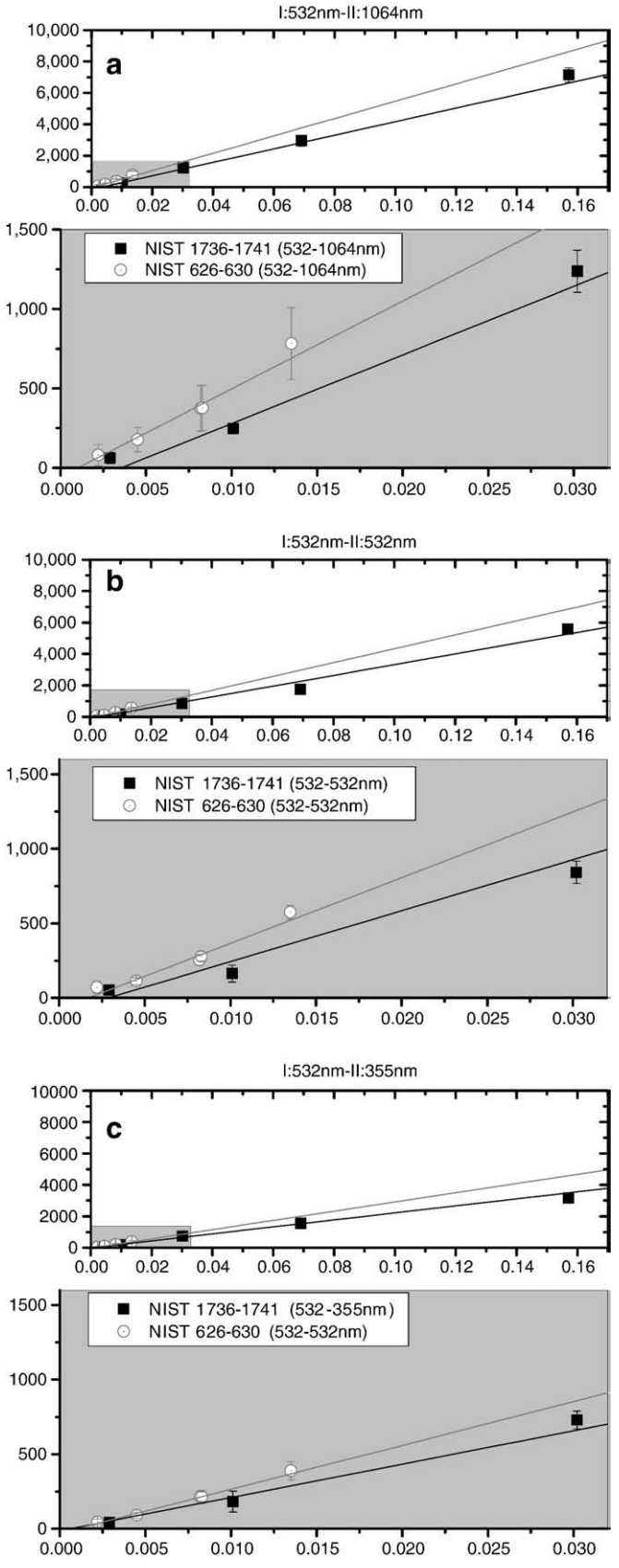

Fig. 6. Lead (Pb) calibration curves from each set of alloy standards (NIST 626–630 and NIST 1737–1741) using double pulse mode (signals are the average of 100 measurements).

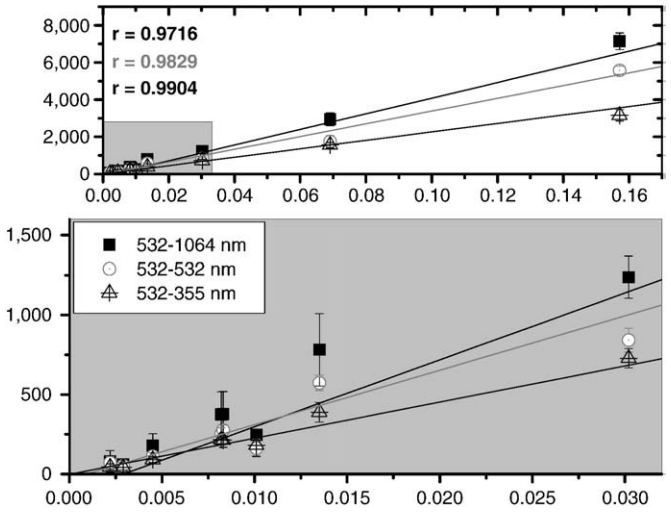

Fig. 7. Lead (Pb) calibration curves from two sets of alloy standards (NIST 626–630 and NIST 1737–1741) using double pulse mode (signals are the average of 100 measurements).

The presence of these elements (aluminum and/or copper) seems to favor the emission of lead from series NIST 626–630 compared to series NIST 1737–1741 based on the higher sensitivity of all the calibration curves, Table 4.

Lead calibration curves were established from other metallic standards with a different matrix (bronze), using the same experimental conditions. Table 2, shows the bronze series standard reference materials from British Chemical Standards (BCS). Fig. 8 shows the calibration curves produced after ablation with the three wavelength combinations for the standard series BCS 551–556. Analogous behavior to the zinc based samples in terms of the increase sensitivity was observed when using the 1064 nm as a second pulse. However, lower sensitivity compared to the zinc base standards also was measured, Table 5.

The major elements in these samples are copper and tin, which may quench lead emission from the plasma. For example, samples BCS 556 (0.16%) and NIST 1741 (0.1571%) contain similar lead concentrations. However, under the same experimental conditions, the lead emission intensity was stronger from the sample NIST 1741; up

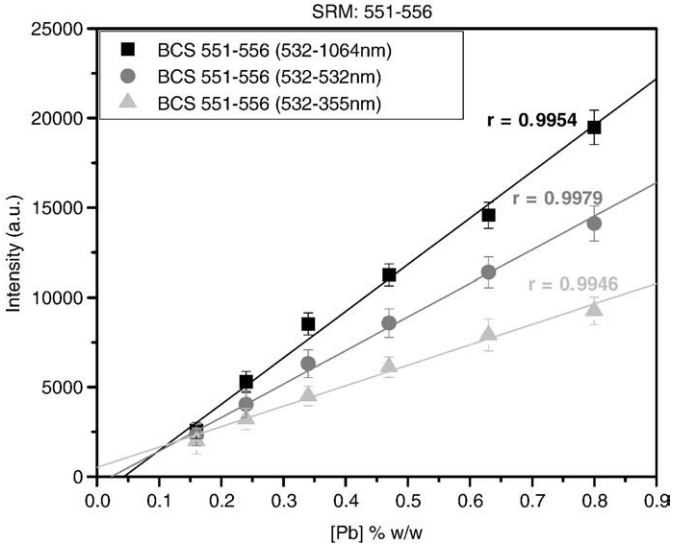

Fig. 8. Lead (Pb) calibration curves from the alloy standard series BCS 551–556, using double pulse mode (signals are the average of 100 measurements).

Table 5
Calibration curve parameters and limit of detection (L.O.D.) for the DP-LIBS approach of the series NIST17xx–6xxand BCS 551–556

Wavelength	slope ± sd	r ± sd	L.O.D (%)	Mode	RM's
532–1064	25922 ± 1265	0.9954 ± 1.0	0.0589	DP	551–556
532–532	18699 ± 1482	0.9979 ± 0.4	0.2378	DP	551–556
532–355	11417 ± 1355	0.9946 ± 0.4	0.1609	DP	551–556
532–1064	42043 ± 2177	0.9716 ± 1.7	0.0018	DP	17xx–6xx
532–532	34217 ± 1235	0.9829 ± 1.8	0.0014	DP	17xx–6xx
532–355	22692 ± 129	0.9904 ± 0.9	0.0017	DP	17xx–6xx

to 3 times compared to the emission intensity from BCS 556. Ismail et al [41] calculated that under the same experimental condition, the higher the ionization potential of the major element of the alloy, the higher is the plasma temperature. From this hypothesis, the hotter plasma (and higher sensitivity) should be produced by the series NIST 1737–1741 since its major element zinc (~99.5%) possess an ionization potential of 9.39 V with negligible amounts of aluminum (~0.4%). Following by standard series NIST 626–630, also with zinc as a major element (~95%) and aluminum (IP 5.99 V) as minor constituent (4.3%), and BCS 551–556 series with copper (IP 7.73 V) and tin (IP 7.34 V) as a major elements.

As predicted, BCS 511–566 provide calibration curves with the poorest sensitivity, most likely due to the lowest plasma temperature. Sensitivities for the other two series of standards shows otherwise, in which NIST 626–630 presents the highest sensitivity even though zinc concentration is lower compared to the concentration in NIST 1737–1741. Even though the complexity of these samples does not allow us to depict a definitive picture of these findings, it can be speculated that the amount aluminum present in the standard series NIST 626–630 (4.3%, IP 5.99 V) plays a key role in favoring the lead signal intensity emission under these experimental conditions.

As in Fig. 6, Fig. 9a, b and c show the calibration curves for each combination of wavelengths for the series NIST 1737–1741, and BCS 551–556. The highlighted regions show the differences between the slopes of the calibration curves obtained for each series. Also from these plots, samples with different matrices cannot be combined to establish extended calibration curves under these experimental conditions. However, a reduction of the matrix effect (based on the higher correlation coefficient of the calibration curve using the combined standards) was obtained when using the combination of wavelengths: I:532 nm–II:355 nm (r=0.9916) (Fig. 10). The correlation coefficient as in Fig. 6 also decreased with the increase of the second pulse wavelength: I:532 nm–II532 nm (r=0.9832), and I:532 nm–II1064 nm (r=0.9824).

These data demonstrate that the matrix-matched requirement, which is a well known limitation of nanosecond laser ablation, can be partially reduced by using double pulse mode. Further improvement of the calibration curve parameters may be possible by using an internal standard to correct for experimental fluctuation.

4. Conclusion

Under the conditions of this study, lead (Pb) emission intensity (atomic line 405.78 nm) was dependent on the sample matrix for double pulse (DP)-laser induced breakdown spectroscopy (LIBS) in collinear configuration. For all the conditions studied, the series of standard samples NIST 626–630 ("$Zn_{95}Al_4Cu_1$") with concentration of the major element zinc of about 95% and higher concentration of minor elements such as aluminum and copper, produced calibration curves with higher sensitivity than the calibration curves produced from NIST 1737–1741 ("$Zn_{99.5}Al_{0.5}$") in which zinc is almost 99.5% of the sample in average, and the series BCS 551–556 ("$Cu_{87}Sn_{11}$") with copper and tin as major elements. These differences in sensitivities

could be the product of different plasma temperatures caused by the differing ionization potential of the major elements and contribution from minor and trace elements.

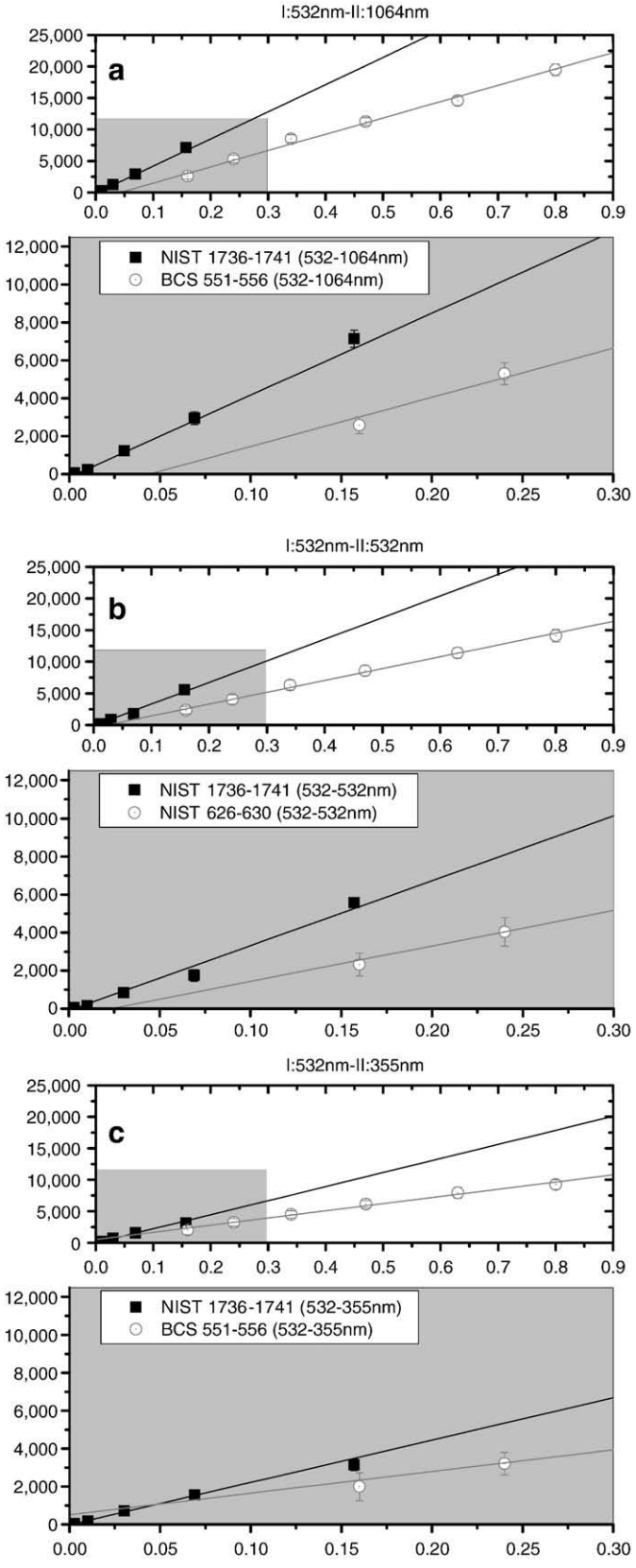

Fig. 9. Lead (Pb) calibration curves of each set of alloy standards (NIST 1737–1741 and BCS 551–556) using double pulse mode (signals are the average of 100 measurements).

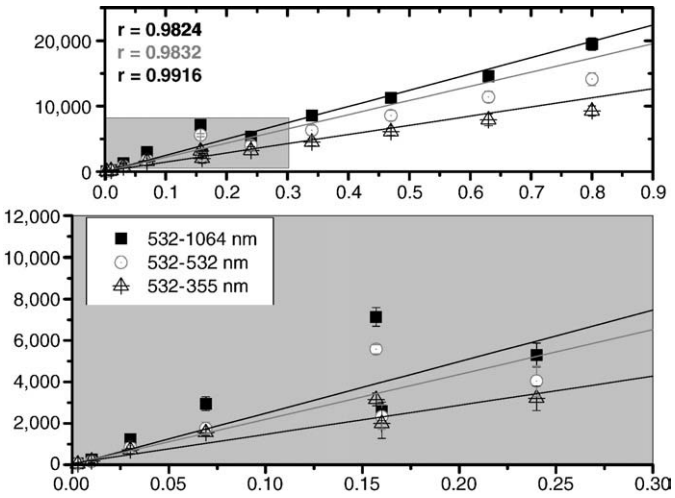

Fig. 10. Lead (Pb) calibration curves from two sets of alloy standards (NIST 1737–1741 and BCS 551–556) using double pulse mode (signals are the average of 100 measurements).

Improvements in sensitivity of double and limit of detection of one order of magnitude are achieved when using the double pulse approach for all the wavelength combinations, compared to the single pulse approach. The wavelength combination I:532 nm=II:1064 nm provides the best sensitivity but the worst reproducibility; while the combination I:532 nm=II:355 nm provides the best reproducibility and the lowest sensitivity of the double pulse approach, but still twice better sensitivity than the single pulse approach. Also, a reduction of the matrix-matched requirement based on the higher correlation coefficient (r) of the calibration curves built using all the standards is reported when the combination of wavelengths I:532 nm–II355 nm was used. The lowest limit of detection of 0.0017% is reported by using two of the series of standards reference materials together and the combination of wavelengths I:532 nm–II355 nm.

Acknowledgements

This work was supported by the Office of Science, Office of Basic Energy Sciences, Chemical Sciences, Geosciences, and Biosciences Division, and the Deputy Administrator for Defense Nuclear Nonproliferation, Research and Development of the U.S. Department of Energy under Contract No. DE-AC02-05CH11231.

V. Piscitelli S, M. A. Martínez L., and A. J. Fernández C., also thank the Consejo de Desarrollo Cientifico y Humanistico (CDCH) of the Central University of Venezuela under Grant 03-00-5881-2007.

References

[1] K. Melessanaki, M. Mateo, S.C. Ferrence, P.P. Betancourt, D. Anglos, The application of LIBS for the analysis of archaeological ceramic and metal artifacts, Appl. Surf. Sci. 197–198 (9-30-2002) 156–163.
[2] S. Acquaviva, M.L. De Giorgi, C. Marini, R. Poso, Elemental analyses by laser induced breakdown spectroscopy as restoration test on a piece of ordnance, J. Cult. Herit. 5 (2004) 365–369.
[3] J. Anzano, M.E. Casanova, M.S. Bermudez, R.J. Lasheras, Rapid characterization of plastics using laser-induced plasma spectroscopy (LIPS), Polym. Test. 25 (2006) 623–627.
[4] A. Brysbaert, K. Melessanaki, D. Anglos, Pigment analysis in Bronze Age Aegean and Eastern Mediterranean painted plaster by laser-induced breakdown spectroscopy (LIBS), J. Archaeol. Sci. 33 (2006) 1095–1104.
[5] F. Colao, R. Fantoni, V. Lazic, A. Paolini, F. Fabbri, G.G. Ori, L. Marinangeli, A. Baliva, Investigation of LIBS feasibility for in situ planetary exploration: an analysis on Martian rock analogues, Planet. Space Sci. 52 (2004) 117–123.
[6] D.C.S. Beddows, O. Samek, M. Liska, H.H. Telle, Single-pulse laser-induced breakdown spectroscopy of samples submerged in water using a single-fiber light delivery system, Spectrochim. Acta Part B 57 (9-13-2002) 1461–1471.
[7] C.M. Davies, H.H. Telle, D.J. Montgomery, R.E. Corbett, Quantitative analysis using remote laser-induced breakdown spectroscopy (LIBS), Spectrochim. Acta Part B 50 (1995) 1059–1075.

[8] C. Lopez-Moreno, S. Palanco, J.J. Laserna, Quantitative analysis of samples at high temperature with remote laser-induced breakdown spectrometry using a room-temperature calibration plot, Spectrochim. Acta Part B 60 (8-31-2005) 1034–1039.
[9] A.I. Whitehouse, J. Young, I.M. Botheroyd, S. Lawson, C.P. Evans, J. Wright, Remote material analysis of nuclear power station steam generator tubes by laser-induced breakdown spectroscopy, Spectrochim. Acta Part B 56 (6-29-2001) 821–830.
[10] R. Nyga, W. Neu, Double pulse technique for optical emission spectroscopy of ablation plasmas of samples in liquids, Opt. Lett. 18 (1993) 747–749.
[11] F. Cignoli, S. Benecchi, G. Zizak, Double pulse technique for the evaluation of the saturation parameter in single-shot laser induced fluorescence measurements: an application to lead in a flame, Spectrochim. Acta Part B 50 (1995) 847–855.
[12] L. St-Onge, M. Sabsabi, P. Cielo, Analysis of solids using laser-induced plasma spectroscopy in double-pulse mode, Spectrochim. Acta Part B 53 (3-30-1998) 407–415.
[13] F. Colao, L. Fornarini, V. Lazic, R. Fantoni, Double pulse laser induced plasma spectrometry on metallic alloys, Communication, 2002.
[14] A. Kumar, F.Y. Yueh, J.P. Singh, Double-pulse laser-induced breakdown spectroscopy with liquid jets of different thicknesses, Appl. Opt. 42 (10-20-2003) 6047–6051.
[15] M. Corsi, G. Cristoforetti, M. Giuffrida, M. Hidalgo, S. Legnaioli, V. Palleschi, A. Salvetti, E. Tognoni, C. Vallebona, Three-dimensional analysis of laser induced plasmas in single and double pulse configuration, Spectrochim. Acta Part B 59 (5-21-2004) 723–735.
[16] A. De Giacomo, M. Dell'Aglio, F. Colao, R. Fantoni, Double pulse laser produced plasma on metallic target in seawater: basic aspects and analytical approach, Spectrochim. Acta Part B 59 (2004) 1431–1438.
[17] C. Gautier, P. Fichet, D. Menut, J.L. Lacour, D. L'Hermite, J. Dubessy, Study of the double-pulse setup with an orthogonal beam geometry for laser-induced breakdown spectroscopy, Spectrochim. Acta Part B 59 (7-30-2004) 975–986.
[18] P.A. Benedetti, G. Cristoforetti, S. Legnaioli, V. Palleschi, L. Pardini, A. Salvetti, E. Tognoni, Effect of laser pulse energies in laser induced breakdown spectroscopy in double-pulse configuration, Spectrochim. Acta Part B 60 (2005) 1392–1401.
[19] V.I. Babushok, F.C. De Lucia, J.L. Gottfried, C.A. Munson, A.W. Miziolek, Double pulse laser ablation and plasma: laser induced breakdown spectroscopy signal enhancement, Spectrochim. Acta Part B 61 (2006) 999–1014.
[20] C. Gautier, P. Fichet, D. Menut, J. Dubessy, Applications of the double-pulse laser-induced breakdown spectroscopy (LIBS) in the collinear beam geometry to the elemental analysis of different materials, Spectrochim. Acta Part B 61 (2006) 210–219.
[21] G. Cristoforetti, S. Legnaioli, L. Pardini, V. Palleschi, A. Salvetti, E. Tognoni, Spectroscopic and shadowgraphic analysis of laser induced plasmas in the orthogonal double pulse pre-ablation configuration, Spectrochim. Acta Part B 61 (2006) 340–350.
[22] M.A. Ismail, G. Cristoforetti, S. Legnaioli, L. Pardini, V. Palleschi, A. Salvetti, E. Tognoni, M.A. Harith, Comparison of detection limits, for two metallic matrices, of laser-induced breakdown spectroscopy in the single and double-pulse configurations, Anal. Bioanal. Chem. 385 (2-13-2006) 316–325.
[23] J. Uebbing, J. Brust, W. Sdorra, F. Leis, K. Niemax, Reheating of a laser-produced plasma by a second pulse laser, Appl. Spectrosc. 45 (11-1-1991) 1419–1423.
[24] C. Gautier, P. Fichet, D. Menut, J.L. Lacour, D.L. L'Hermite, J. Dubessy, Quantification of the intensity enhancements for the double-pulse laser-induced breakdown spectroscopy in the orthogonal beam geometry, Spectrochim. Acta Part B 60 (2005) 265–276.
[25] V. Lazic, F. Colao, R. Fantoni, V. Spizzichino, Laser-induced breakdown spectroscopy in water: improvement of the detection threshold by signal processing, Spectrochim. Acta Part B 60 (2005) 1002–1013.
[26] A. De Giacomo, M. Dell'Aglio, F. Colao, R. Fantoni, V. Lazic, Double-pulse LIBS in bulk water and on submerged bronze samples, Appl. Surf. Sci. 247 (2005) 157–162.
[27] A. Santagata, A. De Bonis, P. Villani, R. Teghil, G.P. Parisi, Fs/ns-dual-pulse orthogonal geometry plasma plume reheating for copper-based-alloys analysis, Appl. Surf. Sci. 252 (4-30-2006) 4685–4690.
[28] L. St-Onge, V. Detalle, M. Sabsabi, Enhanced laser-induced breakdown spectroscopy using the combination of fourth-harmonic and fundamental Nd:YAG laser pulses, Spectrochim. Acta Part B 57 (1-9-2002) 121–135.
[29] A. Ciucci, M. Corsi, V. Palleschi, S. Rastelli, A. Salvetti, E. Tognoni, New procedure for quantitative elemental analysis by laser-induced plasma spectroscopy, Appl. Spectrosc. 53 (1999) 960–964.
[30] C. Lopez-Moreno, S. Palanco, J.J. Laserna, Calibration transfer method for the quantitative analysis of high-temperature materials with stand-off laser-induced breakdown spectroscopy, J. Anal. At. Spectrom. 20 (2005) 1275–1279.
[31] P. Yaroshchyk, D. Body, R.J.S. Morrison, B.L. Chadwick, A semi-quantitative standard-less analysis method for laser-induced breakdown spectroscopy, Spectrochim. Acta Part B 61 (2006) 200–209.
[32] B. Salle, J.L. Lacour, P. Mauchien, P. Fichet, S. Maurice, G. Manhes, Comparative study of different methodologies for quantitative rock analysis by Laser-Induced Breakdown Spectroscopy in a simulated Martian atmosphere, Spectrochim. Acta Part B 61 (2006) 301–313.
[33] M. Corsi, G. Cristoforetti, M. Hidalgo, S. Legnaioli, V. Palleschi, A. Salvetti, E. Tognoni, C. Vallebona, Double pulse, calibration-free laser-induced breakdown spectroscopy: a new technique for in situ standard-less analysis of polluted soils, Appl. Geochem. 21 (2006) 748–755.
[34] V.S. Burakov, S.N. Raikov, Quantitative analysis of alloys and glasses by a calibration-free method using laser-induced breakdown spectroscopy, Spectrochim. Acta Part B 62 (2007) 217–223.
[35] G. Galbács, I.B. Gornushkin, B.W. Smith, J.D. Winefordner, Semi-quantitative analysis of binary alloys using laser induced breakdown spectroscopy and new calibration approach based on linear correlation, Spectrochim. Acta Part B 56 (2001) 1159–1173.
[36] X.L. Mao, A.C. Ciocan, O.V. Borisov, R.E. Russo, Laser ablation processes investigated using inductively coupled plasma atomic emission spectroscopy (ICP-AES), Appl. Surf. Sci. 129 (1998) 262–268.
[37] X.L. Mao, O.V. Borisov, R.E. Russo, Enhancements in laser ablation inductively coupled plasma-atomic emission spectrometry based on laser properties and ambient environment, Spectrochim. Acta Part B 53 (5-29-1998) 731–739.
[38] A. Bogaerts, Z. Chen, Effect of laser parameters on laser ablation and laser-induced plasma formation: a numerical modeling investigation, Spectrochim. Acta Part B 60 (2005) 1280–1307.
[39] L.M. Cabalin, J. Laserna, Experimental determination of laser induced breakdown thresholds of metals under nanosecond Q-switched laser operation, Spectrochim. Acta Part B 53 (1998) 723–730.
[40] A. Bogaerts, Z. Chen, D. Autrique, Double pulse laser ablation and laser induced breakdown spectroscopy: a modeling investigation, Spectrochim. Acta Part B 63 (2008) 746–754.
[41] M.A. Ismail, H. Imam, A. Elhassan, W.T. Youniss, M.A. Harith, LIBS limit of detection and plasma parameters of some elements in two different metallic matrices, J. Anal. At. Spectrom. 19 (2004) 489–494.